Optical and radiocarbon ages of stacked paleosols and dune sands in the Nebraska Sand Hills, USA

R.J. Goble*, Joseph A. Mason, David B. Loope, James B. Swinehart

Department of Geosciences, University of Nebraska-Lincoln, 214 Bessey Hall, Lincoln, NE, 68588-0340, USA

Accepted 30 September 2003

Abstract

Optical ages for eolian sands from the Nebraska Sand Hills indicate periods of extensive eolian activity at ca 115 ± 25, 840 ± 70, 2300 ± 240, and 3560 ± 340 a. Activity was also noted at single sampling locations at ca 6180 ± 370, 8430 ± 510 and 13110 ± 800 a. Many of these ages are similar to those noted by earlier authors. Optical ages from samples collected within paleosols indicate shorter and possibly less extensive periods of eolian activity at approximately 1220 ± 150, 1590 ± 110, and possibly 1950 ± 150 a, during which the paleosol sands accumulated. What was originally interpreted as a single 1.2 m thick paleosol is shown by optical dating to consist of three or more welded soils developed within eolian sands with optical ages of ca 3800 ± 240, 2740 ± 240, 1560 ± 110, and possibly 1930 ± 140 a, each of which match eolian pulses recognized elsewhere. Scatter in some optical ages is attributable to intersection of sand-filled rodent burrows extending in outcrop 1.5 m below the contact between paleosol and overlying topset beds. A 5310 ± 360 a optical age for one probable intersected burrow provides evidence for upward or lateral transport of older sands.

© 2003 Elsevier Ltd. All rights reserved.

1. Introduction

In the episodically active eolian dune fields of the Great Plains, buried soils provide crucial evidence for periods of time during which the dunes were grass-covered and immobile (e.g. Ahlbrandt et al., 1983; Loope et al., 1995; Muhs et al., 1996; Arbogast and Johnson, 1998; Holliday, 2001). In earlier work, organic matter preserved in these paleosols provided key evidence reconstructing the chronology of dune field activity, because radiocarbon dating of buried soil humus provides limiting ages for eolian sand above or below the soil. Episodes of sand transport can be dated directly with optical dating techniques (Stokes and Swinehart, 1997; Aitken, 1998; Forman et al., 2001), and optical dating potentially can provide better resolution of dune field chronology than is possible with radiocarbon dating of soil organic matter. Although the paleosols within Great Plains dune fields are still of interest as a source of information on potentially lengthy periods of dune field stability, optical dating can also provide important new insight into the stratigraphic and paleoenvironmental significance of the paleosols.

Buried soils in the Nebraska Sand Hills, the largest Great Plains dune field, display morphological variation suggesting variation in either the duration of pedogenesis, or the environmental conditions in which the soil formed. Virtually all surface and buried upland soils in the Sand Hills have a simple A–C or A–AC–C horizon sequence (Kuzila, 1990), but the A horizons of paleosols vary widely in thickness and color. The A horizons of most surface soils and many paleosols are thin (< 20 cm) and light-colored, but some buried A horizons are much thicker (up to 1.2 m) and darker colored (Fig. 1, Paleosol 2). The thick, dark-colored paleosols could represent soil formation beneath a land surface under climatic conditions favoring high primary productivity, slow organic matter turnover, and deep bioturbation, or during long periods of dune field stability. Alternatively, they could be thick cumulative A horizons that formed through slow sedimentation accompanied by ongoing organic matter accumulation (Birkeland, 1999). We will demonstrate that they can also represent a third

*Corresponding author. Tel.: +1-402-472-2649; fax: +1-402-472-4917.

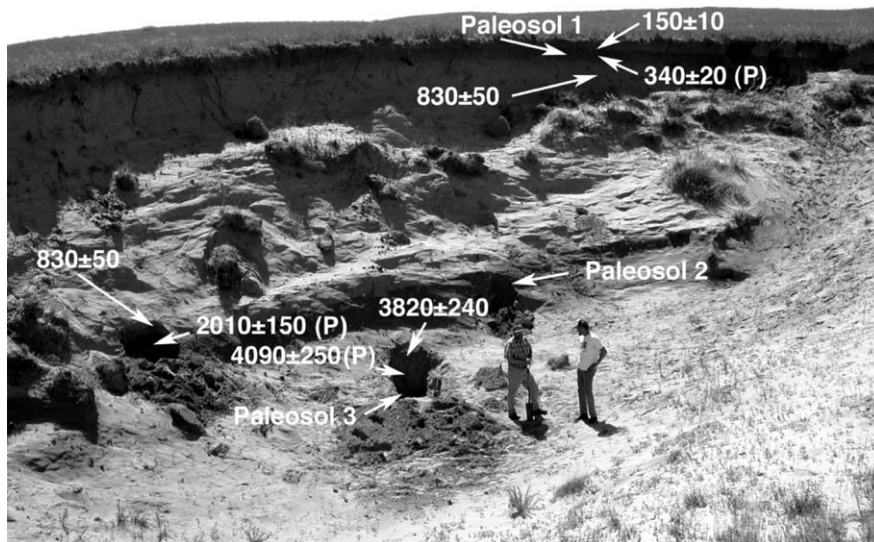*E-mail address:* rgoble2@unl.edu (R.J. Goble).

Fig. 1. Yao's Blowout, Nebraska Sand Hills. Paleosols are labeled and optical ages indicated. (P) Designates optical ages from paleosols.

alternative, welded paleosols (Ruhe and Olson, 1980) developed on sediment deposited during a few discrete periods of sedimentation.

Optical age determinations at multiple depths within a soil can be used to test these alternative explanations for thick horizon development. Most burrowing animals bring soil to the surface (Hole, 1981) where it is exposed to light, bleaching grains and resetting their optical ages. The bleached grains are then buried by later-excavated soil, and can ultimately be cycled downward toward the base of the bioturbated zone. Partial bleaching of grains exposed at the surface by bioturbation can potentially be detected with single aliquot techniques of optical dating (Li, 1994; Olley et al., 1998; Murray and Olley, 1999; Clarke and Rendell, 2000; Colls et al., 2001; Bailey et al., 2002). Cumulative A horizons developed through slow but steady sediment deposition or by slow bioturbation should yield a regularly decreasing optical age profile. On the other hand, if a cumulative A horizon develops through a few brief episodes of sedimentation with little deep bioturbation, the result should be a stepped optical age profile.

In this study, we applied optical dating at several sites in which paleosols occur within eolian sands, together with radiocarbon dating of organic matter in the paleosols. One of our objectives was to compare age estimates for episodes of eolian activity based on optical dating of undisturbed eolian sand and on radiocarbon dating of underlying or bracketing paleosols.

Other objectives focus on interpretation of paleosols. First, we sought to determine whether an optical age from a buried A horizon is best interpreted as (a) an estimate of the age of the initial sand deposit in which the paleosol formed; (b) an estimate of the time of A horizon burial, due to resetting of the optical age of the sand to the time of burial during bioturbation; or (c) an intermediate age between deposition and burial, because of incomplete bleaching of the sand during bioturbation. Second, we investigated whether closely spaced optical age determinations within a paleosol can be used to distinguish among (a) cumulative soil development on a slowly aggrading land surface, (b) bioturbation beneath a non-aggrading land surface, and (c) punctuated episodes of soil development that follow each of a series of discrete sedimentation events.

2. Methods

2.1. Sample locations

Samples were collected at three locations in the Nebraska Sand Hills (A, B, and C; Fig. 2). These consist of "Mick's Slide" on the north bank of the Middle Loup River (Location A, Fig. 2; 42°23′N, 101°01′W) and nearby "Yao's Blowout" approximately one-half kilometer south of the Middle Loup River (Location A, Fig. 2; 42°05′N, 101°22′W; see also Fig. 1), "Briefcase Wayside" on the east side of Nebraska Highway 97 north of Mullen (Location B, Fig. 2; 42°23′N, 101°01′W), and the north and south sides of "Kroeger Blowout" northwest of Valentine (Location C, Fig. 2; 42°57′N, 101°9′W). The most intensive paleosol study was conducted at "Yao's Blowout".

Single paleosols are exposed at "Mick's Slide", a location previously sampled by Stokes and Swinehart (1997), and at "Briefcase Wayside". Three paleosols are exposed in the south face of the "Kroeger Blowout". However, the lowermost of these paleosols is missing from the north side of the blowout due to truncation.

Three inclined paleosols and overlying topset beds are exposed in "Yao's Blowout" on the north (stoss) slope
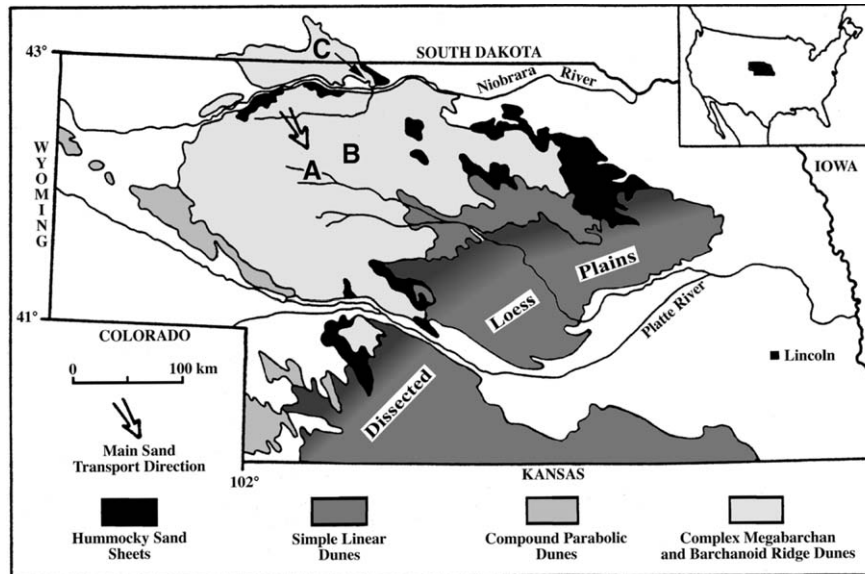
Fig. 2. Study sites in the Nebraska Sand Hills. Yao's Blowout and Mick's Slide are at location A, Briefcase Wayside at location B, and Kroeger Blowout at location C (modified from Stokes and Swinehart, 1997).

of a large barchanoid dune. Where sampled, the tops of the three paleosols lie at depths of approximately 0.5, 6.5, and 9.25 m. The upper and middle paleosols are approximately 0.3 and 1.2 m in thickness; the lowest is not fully exposed. We initially interpreted the middle paleosol as having formed beneath a single land surface, and attributed its greater thickness to a long period of dune stability or climatic conditions favoring high primary productivity. We considered it unlikely that this paleosol was a cumulative soil because it is on the north-facing stoss side of a large dune. Under the northerly winds that shaped most Sand Hills dunes (Loope and Swinehart, 2000), Yao's Blowout would be in an erosional setting. Slow net accumulation of sand at this site would likely require sand transport from the dune crest by southerly winds.

Samples for optical dating were collected from eolian sands and paleosols at these three locations (Table 1 and Fig. 3). Samples for radiocarbon dating were also collected from the paleosols (Table 2 and Fig. 3). Subsequently, we decided to test our interpretation of the long-term stability of the middle paleosol at Yao's Blowout by collecting and analyzing a 1-m vertical section through this paleosol (Table 3 and Figs. 3 and 6), as well as an additional horizontal sample from below its base.

2.2. Sampling methods

Samples were collected in 20 cm long, 5 cm diameter aluminum tubes driven horizontally into the unconsolidated sands. The middle paleosol at Yao's Blowout was sampled by driving a 110 cm long, 7.5 cm diameter aluminum tube vertically into the paleosol beginning

9 cm above the top; 28 cm of compaction occurred and has been corrected for in the data. The ends of the sample tubes were immediately sealed to prevent further light exposure. Additional samples were collected for determination of soil water content and for chemical analysis. Samples for radiocarbon dating were collected from the uppermost five centimeters of each paleosol.

2.3. Optical dating preparation and analysis methods

Concentrations of U, Th, and K were determined by inductively coupled plasma-mass spectrometry (ICP-MS), inductively coupled plasma-atomic emission spectrometry (ICP-AES) and X-ray fluorescent spectrometry (XRFS). Sample compositions from individual locations are generally consistent. For example, comparison of chemical analyses carried out by two different laboratories using two techniques for K (ICP-AES and XRFS) and two different laboratories using the same technique for U and Th (ICP-MS) for 22 samples from Yao's Blowout indicates a mean of $1.88 \pm 0.05\%$ K_2O, 4.6 ± 0.5 ppm Th, and 0.90 ± 0.13 ppm U (Tables 1 and 3). These K_2O and U data are within the analytical error of combined flame photometry, neutron activation and gamma-ray spectrometry analyses of three samples from Gudmundsen ranch reported by Stokes and Swinehart (1997); Th data are slightly higher than reported by Stokes and Swinehart (1997). The in situ moisture content, as determined by weight loss on heating, was used in all calculations. The cosmic contribution to the dose rate was calculated using the method of Prescott and Hutton (1994).

All equivalent dose (D_e) determinations were carried out on the quartz fraction separated from a bulk

Table 1
Field and laboratory data, and OSL results

Sample	Depth[a] (m)	In situ moisture content (%)	K$_2$O (%)	Th (ppm)	U (ppm)	D_{cosmic}[b] (Gy a^{-1} × 10^3)	D_{Total} (Gy a^{-1} × 10^3)	D_e (Gy ± 1σ_s)	Aliquots (n)	Age (a ± 1σ)
Yao's Blowout, south of Middle Loup River										
00RJG1	0.4	4.8	1.90	4.8	0.9	0.24	2.19 ± 0.05	0.32 ± 0.01	100	150 ± 10[c]
00RJG2	0.5	4.5	1.91	4.4	0.9	0.24	2.18 ± 0.05	0.74 ± 0.03	18	340 ± 20[e]
00RJG3	1.0	5.3	1.94	4.4	1.0	0.22	2.19 ± 0.05	1.81 ± 0.01	134	830 ± 50
00RJG4	6.3	8.3	1.84	5.6	1.0	0.11	2.03 ± 0.05	1.69 ± 0.04[d]	20	830 ± 50
00RJG5	6.5	7.6	1.82	4.8	0.9	0.11	1.95 ± 0.05	3.91 ± 0.18	14	2010 ± 150[e]
00RJG6	8.5	5.2	1.81	3.5	0.8	0.09	1.85 ± 0.05	7.08 ± 0.12	28	3820 ± 240
00RJG7	9.4	10.2	2.00	5.6	1.4	0.08	2.15 ± 0.06	8.79 ± 0.12	27	4090 ± 250[e]
Mick's Slide, north of Middle Loup River										
00RJG8	15.0	8.4	1.97	4.3	0.9	0.05	1.96 ± 0.05	1.62 ± 0.04	24	830 ± 50
00RJG9	15.4	7.9	1.72	3.9	0.7	0.05	1.70 ± 0.05	2.02 ± 0.06	23	1180 ± 80[e]
Briefcase wayside, Highway 97										
00RJG10	2.0	4.5	1.43	4.0	0.9	0.19	1.74 ± 0.05	1.80 ± 0.05	20	1040 ± 70
00RJG11	2.3	3.5	1.49	3.1	0.7	0.19	1.71 ± 0.04	2.87 ± 0.13	17	1680 ± 120[e]
00RJG12	3.5	4.8	1.47	4.1	0.7	0.16	1.69 ± 0.05	5.50 ± 0.08	32	3250 ± 200
Kroeger Blowout, south side, northwest of Valentine										
00RJG17	1.3	4.3	2.00	5.1	1.1	0.21	2.32 ± 0.05	2.05 ± 0.04	18	880 ± 50
00RJG16	1.7	5.4	1.96	6.1	1.1	0.20	2.31 ± 0.06	2.45 ± 0.04	21	1060 ± 60[e]
00RJG15	6.3	8.7	2.07	7.9	1.6	0.11	2.45 ± 0.07	5.96 ± 0.09	33	2430 ± 150
00RJG14	6.8	10.0	2.02	5.1	1.4	0.11	2.16 ± 0.06	6.09 ± 0.11	30	2820 ± 180[e]
00RJG13	8.4	7.9	2.01	6.3	1.5	0.09	2.29 ± 0.06	8.20 ± 0.15	10	3590 ± 220
Kroeger Blowout, north side, northwest of Valentine										
00RJG22	1.3	3.5	1.91	7.0	1.2	0.21	2.43 ± 0.06	2.05 ± 0.06	15	840 ± 60
00RJG21	1.7	3.9	1.86	7.4	1.2	0.20	2.39 ± 0.06	3.77 ± 0.16	15	1580 ± 110[e]
00RJG20	12.0	5.2	1.84	4.1	1.1	0.06	2.00 ± 0.05	12.36 ± 0.12	31	6180 ± 370
00RJG19	12.3	6.4	2.01	5.7	1.2	0.06	2.20 ± 0.05	18.50 ± 0.28	29	8430 ± 510
00RJG18	18.0	4.3	1.88	6.5	1.2	0.03	2.17 ± 0.05	28.60 ± 0.48	25	13110 ± 800

[a] Depth of sample below current land surface. Samples are arranged in order of increasing depth at each sample location.

[b] Calculated from locational data and depth of burial using the techniques of Prescott and Hutton (1994).

[c] Lowest 5% of aliquots yield an age of 86 ± 12 a. Use of the "leading edge" of the distribution (Lepper et al., 2000) yields an age of 113 ± 25 a, with a thermal transfer component equivalent to 70 ± 31 a; lowering the Preheat temperature to 180°C yields an age of 85 ± 35 a, which still includes a small amount of thermal transfer.

[d] Multiple aliquot additive paleodose is 1.74 Gy, based on 40 disks.
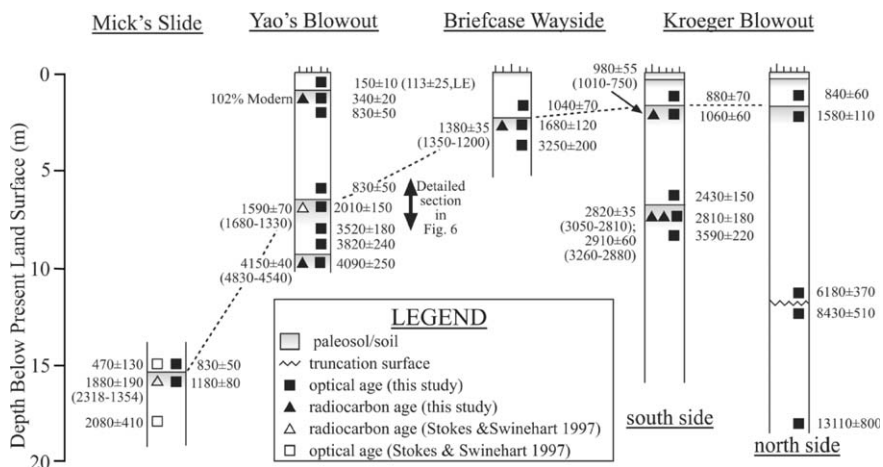
[e] Sample collected from within a paleosol.

Fig. 3. Optical and radiocarbon ages for Mick's Slide, Yao's Blowout, Briefcase Wayside, and Kroeger Blowout. Optical ages are in a, uncalibrated radiocarbon ages in ^{14}C yr BP, and calibrated radiocarbon ages (in parentheses) in cal yr BP.

Table 2
Radiocarbon ages

Field#	Laboratory#	^{14}C age	Calibrated age* range (2σ)	Delta ^{13}C	Locality information
RCJ91-10A	Beta-50438; ETH-9089	2910 ± 60	3260–2880		Kroeger S.-3rd paleosol
RCJ91-11	Beta-50435; ETH-9088	980 ± 55	1010–750		Kroeger S.-2nd paleosol
RCJ00-123	CURL-5321	4150 ± 40	4830–4540	−17.3	Yao's-3rd paleosol
RCJ00-124	CURL-5322	102% modern		−17.4	Yao's-1st paleosol
RCJ00-125	CURL-5323	1380 ± 35	1350–1200	−15.8	Briefcase Wayside
RCJ00-126	CURL-5324	2820 ± 35	3050–2810	−18.5	Kroeger S.-3rd paleosol

*Determined using OxCal v3.5.

Table 3
OSL results from paleosol #2 core, Yao's Blowout

Sample	Depth[a] (cm)	In situ moisture content (%)	K_2O (%)	Th (ppm)	U (ppm)	D_{cosmic} (Gy $a^{-1} \times 10^3$)	D_{Total} (Gy $a^{-1} \times 10^3$)	D_e (Gy $\pm 1\sigma_S$)	Aliquots (n)	Age ($a \pm 1\sigma$)
00RJG23	−3.4	4.72	1.89	4.2	0.8	0.11	2.00 ± 0.05	1.73 ± 0.03	16	860 ± 50
00RJG24	8.5	6.54	1.90	4.6	0.9	0.11	2.01 ± 0.05	2.62 ± 0.05	21	1300 ± 80
00RJG25	15.3	7.50	1.90	4.4	0.9	0.11	2.04 ± 0.05	3.05 ± 0.12	17	1540 ± 110
00RJG26	22.2	7.55	1.95	4.8	0.9	0.11	2.04 ± 0.05	3.14 ± 0.08	17	1540 ± 100
00RJG27	29.0	7.59	1.81	4.6	0.9	0.11	1.92 ± 0.05	3.69 ± 0.12	22	1920 ± 130
00RJG28	35.8	7.78	1.82	4.2	0.8	0.11	1.87 ± 0.05	3.05 ± 0.14	18	1630 ± 120
00RJG29	42.6	7.77	1.83	4.4	0.8	0.11	1.89 ± 0.05	3.76 ± 0.13	20	1990 ± 140
00RJG30	49.4	7.91	1.83	4.4	0.9	0.10	1.91 ± 0.05	5.63 ± 0.17	21	2940 ± 200
00RJG31	56.2	7.94	1.88	4.4	0.9	0.10	1.95 ± 0.05	10.33 ± 0.30	26	5310 ± 350
00RJG32	63.0	7.47	1.86	4.2	0.8	0.10	1.91 ± 0.05	5.20 ± 0.23	24	2730 ± 200
00RJG33	69.9	7.38	1.94	4.6	0.9	0.10	2.02 ± 0.05	5.28 ± 0.18	20	2620 ± 180
00RJG34	76.7	8.35	1.93	5.0	0.9	0.10	2.01 ± 0.05	5.19 ± 0.11	21	2580 ± 160
00RJG35	83.5	7.63	1.86	4.4	0.8	0.10	1.91 ± 0.05	5.57 ± 0.16	21	2910 ± 190
00RJG36	90.3	7.81	1.84	4.6	0.9	0.10	1.93 ± 0.05	5.32 ± 0.15	23	2760 ± 180
00RJG37	135	7.94	1.88	4.3	0.9	0.10	1.93 ± 0.05	7.35 ± 0.08	24	3800 ± 230

[a] Depth of sample below the top of paleosol 2; 00RJG23 is 3.4 cm above the paleosol. Paleosol #2 is 6.5 m below the current land surface.

sediment sample under subdued amber light conditions. For the 110 cm long, 7.5 cm diameter sample tube, approximately 4 cm of mixed sand at the contact between the paleosol and the overlying eolian sand was discarded and the remainder sampled in 5 cm long sections (6.8 cm after correction for compaction).

Separation procedures included HCl (1 N) treatment to remove carbonates, wet sieving to extract the 90–125 μm fraction, heavy liquid ($\rho = 2.70\,g\,cm^{-3}$) separation to remove heavy minerals, etching using both HF (48%) and H_2SiF_6 (23%) to remove feldspars, and resieving. Quartz grains were mounted as monolayers on 9.8 mm diameter aluminum disks using silicone spray (Silkospray). Samples were screened for purity with a binocular microscope, and tested for feldpar contamination using infrared light stimulation.

Most OSL measurements were carried out on a Daybreak Nuclear and Medical Systems reader equipped with green ($\lambda = 514$ nm) and infrared diodes, an EMI 9635Q photomultiplier, UG-11 filters, and an on-plate irradiator with a 100 mCi ^{90}Sr source delivering approximately $0.05\,Gy\,s^{-1}$. Stimulation was by green diodes operated at a power level on the sample of approximately $24.2\,mW\,cm^{-2}$. Some later measurements

were carried out on the same reader upgraded with blue-green diodes. Comparative data for one sample (00RJG3, Table 1) were collected using a RisoTL/OSL-DA-15B reader using blue-green diodes; the means of these measurements were indistinguishable, although the standard deviation for the Riso data was somewhat lower.

Equivalent doses were determined using a single aliquot regenerative (SAR) method (Murray and Roberts, 1998; Murray and Wintle, 2000). For each aliquot, four regenerative doses were used; the fourth repeated the first; test doses (~ 1 Gy) were applied after the natural and each regenerative measurement. A $240^\circ C$, 10 s preheat was used for the natural and regenerative measurements, and a $160^\circ C$, 10 s preheat for the test dose measurements. Signal measurement was at $125^\circ C$. Preheat plateau, dose recovery, and thermal transfer tests were performed on representative samples.

A single saturating exponential was fit to the growth curves to determine the equivalent dose (D_e) corresponding to the natural OSL signal. D_e frequency distributions (Olley et al., 1998, 1999), standardized plots of paleodose vs. signal intensity (Colls et al., 2001), and $D_e - t$ plots (Bailey et al., 2002) were checked for

evidence of partial bleaching. Individual D_e determinations were accepted/rejected based upon recycling ratio, percent error in the D_e determination, and test dose error; a sticking shutter on the Daybreak irradiator also caused some runs to be rejected. D_e errors in Tables 1 and 3 are quoted as one standard error. Error treatment for age calculations follows Aitken and Alldred (1972) and Aitken (1976).

For one sample (00RJG4), an equivalent dose was also determined using a multiple aliquot additive dose method and natural normalization (Aitken, 1995, 1998). Forty aliquots were prepared as described above, and a 160°C, 16-h preheat used (Stokes, 1992, 1994). A single saturating exponential with a linear component was fit to the data (Aitken, 1998). The estimated D_e of 1.74 Gy is just greater than one standard error (± 0.04 Gy) associated with the D_e of 1.69 Gy determined for this sample using the SAR technique (Table 1), but is within one standard deviation.

2.4. Radiocarbon dating preparation and analysis methods

Radiocarbon samples were dry sieved and the silt/clay fraction ($< 62\,\mu m$) submitted for AMS analysis of total organic carbon. The samples were dispersed in hot acid to eliminate carbonates. The radiocarbon ages were calibrated with the program OxCal v. 3.5 using the INCAL98 data (Ramsey, 1995).

3. Results

3.1. Yao's Blowout

Dose rate and D_e data for the initial seven samples from Yao's Blowout are given in Table 1 and Fig. 3. The optical ages are internally consistent, within the error limits. The well-stratified sands that overlie the upper and middle paleosols have ages of 150 ± 10 and 830 ± 50 a; eolian sands above the lowest paleosol have an age of 3820 ± 240 a. The age for the uppermost sands is consistent with a previous multiple aliquot regenerative optical 250 ± 80 a age for sands in Mick's Slide north of the Middle Loup River (Stokes and Swinehart, 1997). Only the sample above the upper paleosol shows evidence of partial bleaching; using the lower 5% D_e's produces an estimated age of 86 ± 12 a ($D_e = 0.19$ Gy). The "Leading Edge" of the distribution (Lepper et al., 2000) yields an age of 113 ± 25 a ($D_e = 0.25$ Gy). Thermal transfer at the 240°C preheat temperature is 0.16 Gy, equivalent to 70 a. Lowering the preheat temperature to 180°C reduces the apparent optical age to 85 ± 35 a; this includes a small amount of thermal transfer. The bioturbated sands within the three paleosols have optical ages of 340 ± 20, 2010 ± 150, and

4090 ± 250 a, as compared to calibrated radiocarbon ages of 1680–1330 (Stokes and Swinehart, 1997) and 4830–4540 cal yr BP for the two lower paleosols (Table 2); one optical age is older and one younger than the comparable radiocarbon ages.

3.2. Mick's Slide

The optical age of 830 ± 50 a determined for eolian sand above the paleosol exposed in Mick's Slide (Table 1 and Fig. 3) is somewhat older than a multiple aliquot optical 470 ± 130 a age previously determined by Stokes and Swinehart (1997), but identical to the 830 ± 50 age determined for eolian sands at Yao's blowout. The optical paleosol age of 1180 ± 80 a is much younger than Stokes and Swinehart's (1997) 2318–1354 cal yr B calibrated radiocarbon age.

3.3. Briefcase wayside

Optical data for the paleosol exposed at Briefcase Wayside, and the sands above and below it are shown in Table 1 and Fig. 3; paleosol radiocarbon data are in Table 2. The 1040 ± 70 and 3250 ± 200 a optical ages for the eolian sands are similar to those for the sands above and below the middle paleosol at Yao's Blowout; error bars on ages from the two localities almost overlap. The optical age of the paleosol (1680 ± 120 a) is significantly older than the corresponding calibrated radiocarbon age of 1350–1200 cal yr BP.

3.4. Kroeger Blowout

Optical ages for samples from Kroeger Blowout are given in Table 1 and Fig. 3; radiocarbon data are in Table 2. Optical ages of 880 ± 50 yr and 840 ± 60 a for the eolian sands below the unsampled upper paleosol on the south and north sides of the blowout are similar to those for eolian sands at Yao's Blowout, Mick's Slide, and Briefcase Wayside. Sands between the second and third paleosol on the south side have an optical age of 2430 ± 150 a, similar to the 2080 ± 410 a multiple aliquot age obtained by Stokes and Swinehart (1997) at Mick's Slide. Sands below the second paleosol have an age of 3590 ± 220 a, similar to the age of the lower sands at Yao's Blowout and Briefcase Wayside and to the 3810 ± 640 a multiple aliquot optical age obtained by Stokes and Swinehart (1997) at nearby Merritt Reservoir. Sands above and below the truncation surface on the north side have ages of 6180 ± 370, 8430 ± 510, and 13110 ± 800 a, older than those found in any other location in this study. The younger of these ages is consistent with a multiple aliquot optical age of 5730 ± 710 yr BP at nearby Merritt Reservoir (Stokes and Swinehart, 1997); the oldest age is consistent with

the 9200–15,000 a ages reported from the megabarchan dunes at Gudmundsen Ranch by Stokes et al. (1999).

Samples from the second paleosol at Kroeger Blowout have optical ages of 1060 ± 60 and 1580 ± 110 a on the south and north sides, respectively. The former is similar to the optical age obtained for the paleosol at Mick's Slide, the latter to optical ages for paleosols exposed at Yao's Blowout and Briefcase Wayside. The calibrated radiocarbon age of this paleosol is 1010–750 cal yr BP (Table 2). The third paleosol on the south side has an optical age of 2820 ± 180 a, intermediate to optical ages of paleosols at Yao's Blowout. The calibrated radiocarbon ages from two successive samples are 3050–2810 (upper) and 3260–2880 (lower) cal yr BP.

3.5. Summary of optical ages, non-paleosol sands

The optical ages from non-paleosol sands sampled in this study are summarized as age probability density functions for the period 0–5000 a in Fig. 4. Optical ages from the paleosols have been omitted, and multiple analyses from a single eolian sequence at the same locality have been given a collective weight equal to that of a single sample. Comparable optical data from Stokes and Swinehart (1997) and Stokes et al. (1999) are also shown; data listed as a range (e.g. 7–8 ka) in the latter have not been included.

The data in Fig. 4 show peaks of eolian activity at 240 ± 90, 500 ± 120, 840 ± 70, 2300 ± 240, and 3560 ± 340 a, with a possible minor period of activity at ca 1030 a at Briefcase Wayside. The ca 240 a optical data from this study show evidence of partial bleaching. Use of the "Leading Edge" technique of Lepper et al. (2000) on the sample in this study indicates an age for this latest period of eolian activity of ca 115 ± 25 a. The eolian activity at ca 500 a is based upon the data of

Stokes and Swinehart (1997) and was not detected in this study nor by Stokes et al. (1999).

Eolian sands from the lower part of Kroeger Blowout on the north side have optical ages of 6180 ± 370, 8430 ± 510, and $13,110 \pm 800$ a. The last two ages correspond to periods of eolian activity reported by Stokes et al. (1999).

3.6. Summary of optical and radiocarbon data, paleosol sands

The optical ages from sands collected from paleosols in this study are summarized in the age probability density functions in Fig. 5. The data show peaks of sand accumulation and/or bioturbation-related exposure to light at 300 ± 30, 1140 ± 100, 1640 ± 110, 1980 ± 180, 2820 ± 180, and 4080 ± 260 a. The ca 1140 and 1640 a optical ages were detected at two and three locations, respectively; the ca 2820 and 4080 a ages are similar to ages determined for non-paleosol samples at the same or other locations in this or the earlier studies.

The radiocarbon data from the paleosols are also summarized in Fig. 5. The data show peaks at 1010–750, 1350–1200, 3050–2810, and 4830–4540 cal yr BP. The two younger radiocarbon peaks are younger than the optical ages determined for the corresponding sands by a few hundred years, consistent with accumulation of organic material following burial of the sand. The 3050–2810 cal yr BP radiocarbon peak almost overlaps the optical peak for the same paleosol. The 4830–4540 cal yr BP radiocarbon peak is significantly older than the optical age of ca 4080 a determined for the same sand. However, the optical ages determined for the sand within and above the paleosol (4090 ± 250 and 3820 ± 240 a, Table 1) are almost identical. This suggests that the sand in the OSL sample collected from the paleosol may have been derived from either the
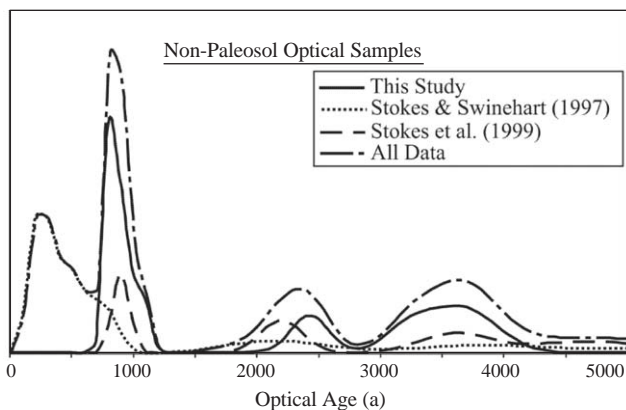

Fig. 4. Optical age probability density functions for eolian, non-paleosol samples, with comparable data from Stokes and Swinehart (1997) and Stokes et al. (1999). Data from Stokes et al. (1999) which quote age ranges rather than mean and standard deviation are omitted (i.e. 7–8 ka).
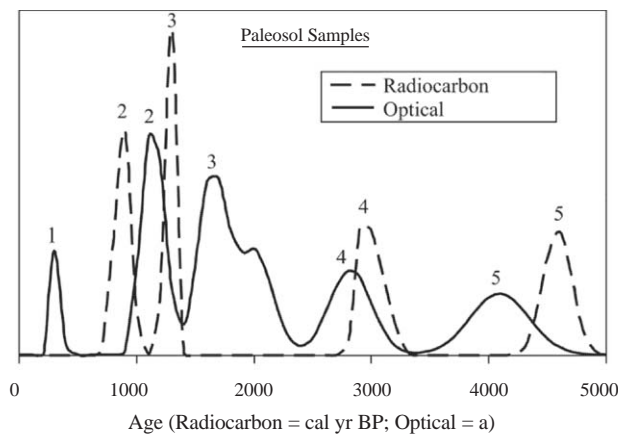

Fig. 5. Optical and calibrated radiocarbon age probability density functions for paleosol samples. Peaks are numbered to indicate corresponding samples.

overlying eolian sand or from a mixture of the paleosol sand and the overlying eolian sand. Possible explanations include mixing due to bioturbation by burrowing rodents or inadvertent sampling of the overlying material due to an irregular contact not visible in the outcrop face.

3.7. Yao's Blowout, detailed paleosol section

Optical ages for the vertical section through the second and thickest of the paleosols in Yao's Blowout are shown in Table 3 and plotted against depth below the top of the paleosol in Fig. 6. An age probability density function constructed from these data is shown directly above the main figure, as are the summed data from Fig. 4 and optical ages from Fig. 5; arrows indicate matches between data sets.

Optical ages from paleosol 2 show a systematic decrease from ca 3800 a in the underlying eolian sands to ca 830 a in the overlying sand, suggesting a possible development as a cumulative profile over a period of ca 3000 yr, as shown by the dashed line. However, the age probability density functions plot for this data set has
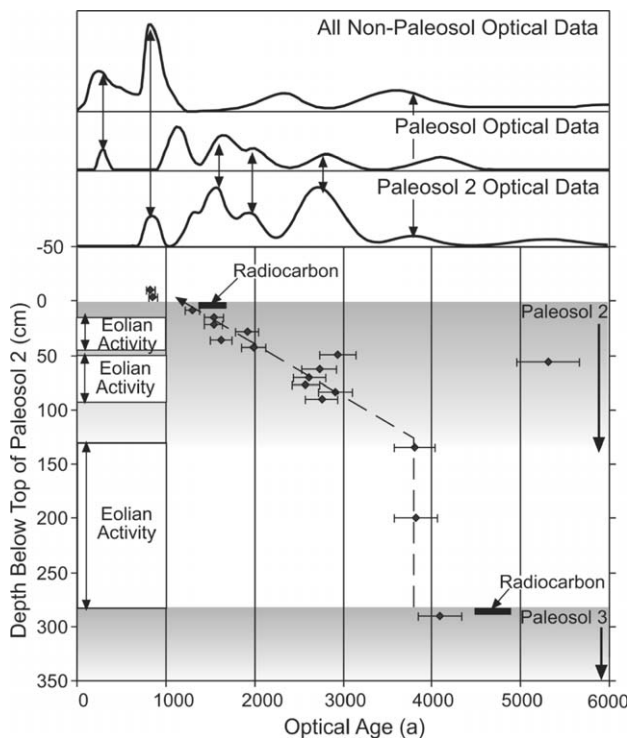

Fig. 6. Optical and radiocarbon ages for the lower two paleosols and adjacent eolian sands at Yao's Blowout. The dashed line indicates the approximate optical ages predicted if paleosol 2 were a cumulative soil profile with systematic bleaching of the sands. The curve directly above shows the age probability density function for these optical ages; arrows indicate correspondence of peak ages with similar data from other Sand Hills paleosols and with non-paleosol optical ages. Interpreted discrete episodes of eolian sedimentation are shown as labeled boxes on the left-hand side of the figure.

prominent peaks at 850 ± 60, 1560 ± 110, 2740 ± 240 and 3800 ± 240 a. The peaks at ca 850 and 3800 a represent the overlying and underlying eolian sands, respectively. That at ca 2740 closely matches an optical age previously determined for one of the Kroeger Blowout paleosol samples; the apparent ca 1560 a age has also been detected in the Sand Hills in optical ages from other paleosols. Minor peaks also occur at 1310 ± 90, 1930 ± 140, and 5310 ± 350 a. The peak at ca 1310 a has been noted in optical ages from paleosols at two other locations, that at ca 5310 a is approximately the same as the 4700 ± 500 a optical age previously determined by Stokes et al. (1999), and is also similar to the 4830–4540 cal yr BP radiocarbon age for paleosol 3, located approximately 2.5 m below this sample.

The recurrence of ca 1300 and 1600 a optical ages for sand in paleosols at several locations within the Sand Hills suggests that these ages represent periods of short-lived but widespread eolian activity. These correspond to two of the periods of pronounced drought during AD 200–370 (1630–1800 a), AD 700–850 (1150–1300 a), and AD 1000–1200 (800–1000 a) noted by Laird et al. (1996) and Fritz et al. (2000) based upon diatom inferred salinity in Moon Lake, North Dakota. The extensive eolian activity in the Sand Hills at ca 850 a corresponds to the third of these three periods.

Based on these data, it appears that paleosol 2 at Yao's Blowout is a "welded" composite of at least three separate paleosols developed on eolian sands deposited at ca 3800, 2700, and 1600 a, with minor eolian activity at approximately 1300 a and possibly 2000 a. The minor peaks centered on ca 1300 and 2000 a probably represent discrete short periods of sand accumulation and associated shallow bioturbation by burrowing rodents. The ca 5300 a optical age may represent the age for more deeply buried eolian sand transported upwards in a rodent burrow and inadvertently sampled in our core. Although no deeply buried sand of similar age was recovered in this study, sand-filled rodent burrows both lighter and darker than the surrounding material were noted and, as noted, the radiocarbon sample from paleosol 3 approximately 2.5 m below this sample is approximately the same age.

The optical ages from the uppermost sand in both lower paleosols at Yao's Blowout are younger than the calibrated radiocarbon age for the same sands (Fig. 6). This is consistent with overturn and exposure of these sands to sunlight, with accompanying bleaching of the optical signal but without removal of the carbon.

4. Summary

The optical ages determined in this and the earlier studies of Stokes and Swinehart (1997) and Stokes et al.

Table 4
Summary of optical and radiocarbon data for the last 5000 years, Nebraska Sand Hills

Eolian optical age (a)	Paleosol optical age (a)[a]	Paleosol radiocarbon age (cal yr BP)
240±90[(3)b,c]		
	310±30[(1)b]	102% modern[b]
470±90[(2)c]		
840±70[(6)b,c,d]		
	1220±150[(3)b]	1010–750[b]
	1590±110[(3)b]	1350–1200[b]
	1950±150[(1)b]	1680–1330[c]
2300±240[(3)b,c,d]		
	2760±230[(2)b]	3050–2810[b,e]
		3260–2880[b,e]
2800–3500[(1)d]		
3560±340[(4)b,d]		
	4090±280[(1)b]	4830–4540[b]
4000±420[(2)b,c]		
4700±490[(1)d]		

Only radiocarbon ages for paleosols sampled in this study are included.
Radiocarbon data are for the paleosol in the same row of the middle column.
Superscript numbers indicate the number of locations at which this age was observed.
[a] Includes all paleosol optical ages shown in Figs. 5 and 6.
[b] This study.
[c] Stokes and Swinehart (1997).
[d] Stokes et al. (1999).
[e] Upper and lower samples from the same paleosol.

(1999) for the last 5000 years of eolian activity in the Nebraska Sand Hills are summarized in Table 4; also included are radiocarbon data for paleosols sampled in this study. The data indicate periods of eolian activity at two or more locations in the Nebraska Sand Hills at 240±90 ("Leading Edge" ~115±25 a), 470±90, 840±70, 2300±240, 3560±340, and 4000±420 a. Additional periods of activity have been noted at a single location in the Sand Hills at ca 2800–3500 and 4700±490 a. Detailed analysis of the middle of three paleosols exposed at Yao's Blowout, in combination with optical ages for paleosols from elsewhere in the Sand Hills, indicates additional short periods of eolian activity at 1220±150 and 1590±110 a. It also provides evidence for short periods of localized sand movement at 2760±230, 4090±280, and 5310±350 a, which may be recorded in the non-paleosol record as well. A possible short period of eolian activity at 1950±150 a is only recorded in the paleosol optical record.

Optical ages also provide evidence for earlier periods of eolian activity in the Sand Hills. Optical ages of 6180±370, 8430±510, and 13,110±800 a recorded in this study may correspond to periods of eolian activity between 7000–8000 and 9200–15,000 a recorded by Stokes et al. (1999).

5. Conclusions

1. Optical ages cluster as episodes. These indicate periods of eolian activity at 115±25 ("Leading Edge" age), 470±90, 840±70, 2300±240, 3560±340, and 4000±420 a; possible additional activity took place at 5310±350, 5730±710, 6180±370, and 8430±510 a, but have not been recorded at more than one Sand Hills locality.
2. The two lowermost samples from Kroeger Blowout, with determined ages of 8430±510 and 13,110±800 a, may correspond to periods of activity between 9200 and 15,000 a recorded by Stokes et al. (1999) at Gudmundsen Ranch.
3. Paleosol optical ages record additional periods of minor and possibly localized activity at 1220±150, 1590±110 and possibly 1950±150 a.

References

Ahlbrandt, T.S., Swinehart, J.B., Maroney, D.G., 1983. The dynamic Holocene dune fields of the Great Plains and Rocky Mountain Basins, USA. In: Brookfield, M.E., Ahlbrandt, T.S. (Eds.), Eolian Sediments and Processes. Elsevier, Amsterdam, pp. 379–406.

Aitken, M.J., 1976. Thermoluminescent age evaluation and assessment of error limits: revised system. Archaeometry 18, 233–238.

Aitken, M.J., 1995. Thermoluminescence Dating. Academic Press, London.

Aitken, M.J., 1998. An Introduction to Optical Dating. Oxford University Press, Oxford.

Aitken, M.J., Alldred, J.C., 1972. The assessment of error limits in thermoluminescent dating. Archaeometry 14, 257–267.

Arbogast, A.F., Johnson, W.C., 1998. Late-Quaternary landscape response to environmental change in south-central Kansas. Annals of the Association of American Geographers 88, 126–145.

Bailey, R.M., Singarayer, J., Ward, S., Stokes, S., 2002. Identification of partial bleaching using D_e as a function of illumination time. Radiation Measurements 37, 511–518.

Birkeland, P.W., 1999. Soils and Geomorphology. Oxford University Press, Oxford.

Clarke, M.L., Rendell, H.M., 2000. The development of a methodology for luminescence dating of Holocene sediments at the land–ocean interface. In: Shennan, I., Andrews, J. (Eds.), Holocene Land–Ocean Interaction and Environmental Change Around the North Sea, Vol. 166, Special Publication. Geological Society, London, pp. 69–86.

Colls, A.E., Stokes, S., Blum, M.D., Straffin, E., 2001. Age limits on the Late Quaternary evolution of the upper Loire River. Quaternary Science Reviews 20, 743–750.

Forman, S.L., Oglesby, R., Webb, R.S., 2001. Temporal and spatial patterns of Holocene dune activity on the Great Plains. Global and Planetary Change 29, 1–29.

Fritz, S.C., Ito, E., Yu, Z., Laird, K.R., Engstrom, D.R., 2000. Hydrologic variation in the Northern Great Plains during the last two millennia. Quaternary Research 53, 175–184.

Hole, F.D., 1981. Effects of animals on soil. Geoderma 25, 75–112.

Holliday, V.T., 2001. Stratigraphy and geochronology of upper Quaternary eolian sand on the Southern High Plains of Texas and New Mexico, United States. Geological Society of America Bulletin 113, 88–108.

Kuzila, M., 1990. Soil associations and series. In: Bleed, A., Flowerday, C. (Eds.), An Atlas of the Sand Hills. Resource Atlas 5a.

Conservation and Survey Division, University of Nebraska-Lincoln, pp. 58–66.

Laird, K.R., Fritz, S.C., Maasch, K.A., Cumming, B.F., 1996. Greater drought intensity and frequency before AD 1200 in the Northern Great Plains, USA. Nature 384, 552–554.

Lepper, K., Agersnap-Larsen, N., McKeever, S.W.S., 2000. Equivalent dose distribution analysis of Holocene eolian and fluvial quartz sands from Central Oklahoma. Radiation Measurements 32, 603–608.

Li, S.-H., 1994. Optical dating: insufficiently bleached sediments. Radiation Measurements 23, 563–568.

Loope, D.B., Swinehart, J.B., 2000. Thinking like a dune field. Great Plains Research 10, 5–35.

Loope, D.B., Swinehart, J.B., Mason, J.P., 1995. Dune-dammed wetlands and buried paleovalleys of the Nebraska Sand Hills: intrinsic vs. climatic controls on the accumulation of lake and marsh sediments. Geological Society of America Bulletin 107, 396–406.

Muhs, D.R., Stafford, T.W., Cowherd, S.D., Mahan, S.A., Kihl, R., Maat, P.B., Bush, C.A., Nehring, J., 1996. Origin of the Late Quaternary dune fields of northeastern Colorado. In: Lancaster, N. (Ed.), Response of Aeolian Processes to Global Change. Geomorphology. Elsevier, Amsterdam, Netherlands, pp. 129–149.

Murray, A.S., Olley, J.M., 1999. Determining sedimentation rates using luminescence dating. GeoResearch Forum 5, 121–144.

Murray, A.S., Roberts, R.G., 1998. Measurement of the equivalent dose in quartz using a regenerative-dose single-aliquot protocol. Radiation Measurements 29, 503–515.

Murray, A.S., Wintle, A.G., 2000. Luminescence dating of quartz using an improved single-aliquot regenerative-dose protocol. Radiation Measurements 32, 57–73.

Olley, J.M., Caitcheon, G.G., Murray, A.S., 1998. The distribution of apparent dose as determined by optically stimulated luminescence in small aliquots of fluvial quartz: implications for dating young samples. Quaternary Science Reviews 17, 1033–1040.

Olley, J.M., Caitcheon, G., Roberts, R.G., 1999. The origin of dose distribution in fluvial sediments, and the prospect of dating single grains from fluvial deposits using optically stimulated luminescence. Radiation Measurements 30, 207–217.

Prescott, J.R., Hutton, J.T., 1994. Cosmic ray contributions to dose rates for luminescence and ESR dating: large depths and long-term time variations. Radiation Measurements 23, 497–500.

Ramsey, B., 1995. Radiocarbon calibration and analysis of stratigraphy, the OxCal program. Radiocarbon 37, 425–430.

Ruhe, R.V., Olson, C.G., 1980. Soil welding. Soil Science 130, 132–139.

Stokes, S., 1992. Optical dating of young sediments using quartz. Quaternary Science Reviews 11, 153–159.

Stokes, S., 1994. The timing of OSL sensitivity changes in a natural quartz. Radiation Measurements 23, 601–606.

Stokes, S., Swinehart, J.B., 1997. Middle- and late-Holocene dune reactivation in the Nebraska Sand Hills, USA. The Holocene 7, 263–272.

Stokes, S., Rich, J., Swinehart, J.B., Loope, D.B., 1999. Holocene timing of megabarchan dune construction in the Nebraska Sand Hills. Geological Society of America, Abstracts with Programs, A-231.